Recognition of the Cell-Wall Binding Site of the Vancomycin-Group Antibiotics by Unnatural Structural Motifs: ^{1}H NMR Studies of the Effects of Ligand Binding on Antibiotic Dimerisation

Patrick Groves,[a] Mark S. Searle,[a] Ines Chicarelli-Robinson[b] and Dudley H. Williams*[,a]
[a] *Cambridge Centre for Molecular Recognition, University Chemical Laboratories, Lensfield Road, Cambridge, CB2 1EW, UK*
[b] *Xenova Ltd., 240 Bath Road, Slough, Berkshire, SL1 4EF, UK*

The synthetic compound *N*-(9-oxofluoren-2-yl)oxamic acid **2** is shown by ^{1}H NMR spectroscopy to bind to the peptide cell-wall recognition site of the vancomycin-group antibiotic, ristocetin A, through hydrogen bonding interactions analogous to those of the cell-wall analogue di-*N*-Ac-L-Lys-D-Ala-D-Ala **1**. The synthetic ligand **2** binds in a highly anti-cooperative manner to the ristocetin dimer (K_{dim} for ristocetin A alone $\approx$ 500 dm^3 mol^{-1}, K_{dim} for ristocetin–**2** complex < 1 dm^3 mol^{-1}, at 300 K), while the natural substrate **1** has a relatively small anti-cooperative effect on dimerisation ($K_{dim} \approx$ 350 dm^3 mol^{-1} at 300 K). Structural and thermodynamic aspects of cooperative/anti-cooperative binding, relevant to the formation of biological aggregates, are examined in this study. ^{1}H NOE data show that the pendant sugars of the antibiotic are 'organised' into a hydrophobic 'wall' with which compound **2** interacts, and which is evidently incompatible with the complementarity required for back-to-back dimerisation. An investigation of the effects on antibiotic dimerisation of a number of substrate analogues, and several ligands which approximate to stepwise truncation of compound **2**, reveals that ligands which introduce unnatural binding interactions with the ring 4 tetrasaccharide and ring 6 ristosamine sugar (particularly hydrophobic interactions with ligand aryl rings), appear to bind highly anti-cooperatively to the dimer, perturbing the subtle complementarity that appears to be synonymous with the formation of the extended aggregate. A number of other vancomycin group antibiotics exhibit positive cooperative effects, suggesting a possible functional role for dimerisation in promoting antibacterial action.

The mode of action of vancomycin-group antibiotics is based on their ability to bind to the cell-wall peptidoglycan of Gram-positive bacteria terminating in the dipeptide -D-Ala-D-Ala.[1] Structure elucidation of the complex of the cell wall analogue *N*-Ac-D-Ala-D-Ala with ristocetin A[2,3] suggests that all of the molecular features of these antibiotics are finely honed through natural selection to promote cell-wall recognition. Molecular complementarity is reminiscent of that found for enzyme–substrate interactions. The ability of the vancomycin group antibiotics to bind cell-wall fragments with high affinity *in vitro* (up to 10^6 dm^3 mol^{-1} in binding constant) presents a paradigm for semi-quantitative studies of molecular recognition in solution.[4–6] Recently, the antibiotics have been shown to form back-to-back homo-dimers,[7–9] with the intriguing possibility that the dimerisation process may have a functional role in promoting antibacterial action by more effectively inhibiting cell-wall synthesis through a chelate-like enhancement of binding to two portions of cell wall.[7–9] Further observations suggest that, in most cases, ligand binding *in vitro* can have the effect of enhancing antibiotic dimerisation by a factor of between 2 (vancomycin) and 100 (eremomycin) for various members of the vancomycin group, adding further complexity and subtlety to the mechanism of action.[9] In this regard, risocetin A appears to be anomolous in that natural substrate binding to the dimer is slightly anti-cooperative (< factor of 2 in K_{dim}). Thus, the dimer–ligand complexes of this family of glycopeptides represent models of extended aggregates with the potential of yielding insights into aspects of cooperative binding phenomena relevant to signalling processes typical of agonist–receptor interactions.

In order to explore greater structural variety in the types of ligands that can be used to probe semi-quantitatively interactions in the binding pocket of ristocetin A, we have designed and synthesised a number of oxamic acid derivatives as alternate templates to the natural substrate **1**.[10] Compound **2** satisfies the criteria for strong binding by i, presenting the correct functional group pattern and geometries for optimum hydrogen bond formation and a complementary binding interaction, ii, having a large hydrophobic surface area to bury into the non-polar residues of the antibiotic binding pocket, and iii, having fewer internal rotations to restrict on binding than the natural substrate.[5] The salient features of the interaction of compounds **1** and **2** with antibiotic hydrogen bond donors and acceptors are represented schematically in Fig. 1.

Compound **2** is found to bind tightly to ristocetin A (Fig. 2), but unexpectedly binds highly anti-cooperatively to the antibiotic dimer (specificity for monomer/dimer > 500). At the concentrations of antibiotic required for detailed NMR studies (a few millimolar), the complex of ristocetin A with compound **2** conveniently exists exclusively in the monomeric form under conditions in which the complex with the natural substrate **1** gives rise to resonances from a mixture of bound antibiotic monomer and two forms of a bound dimer. In this paper, we present an NMR characterisation of the complex of compound **2** with ristocetin A, and present a description of ligand–antibiotic interactions (several of which are unnatural interactions with antibiotic sugar residues that are not found in the complex formed with the natural substrate), that may perturb interactions at the dimer interface and account for the higher affinity of compound **2** for the ristocetin monomer. A semi-quantitative analysis of the relative contributions of portions of the fluorenone moiety to the effects on dimerisation is presented by monitoring the extent of dimer formation in

complexes of a number of ligands approximating to truncated analogues of compound **2** (see Scheme 1).

Results and Discussion

^{1}H *Resonance Assignments.*—^{1}H NMR spectra of ristocetin A in D_2O solution at *ca.* 5 mmol dm^{-3} concentration and 288 K

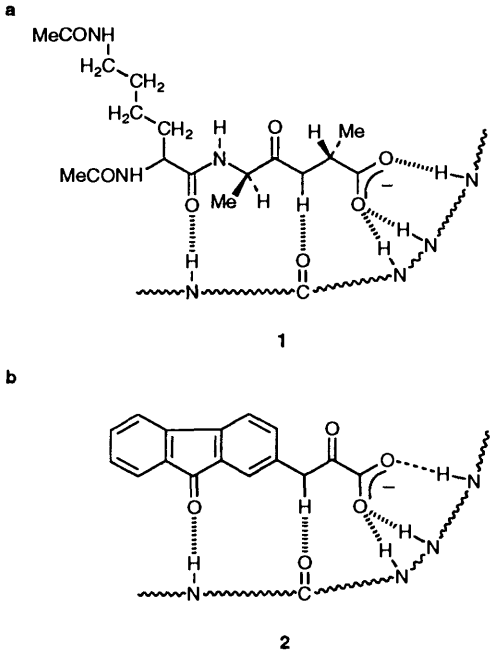

Fig. 1 Schematic illustration of functional group interactions between vancomycin-group antibiotics and **a**, di-*N*-Ac-L-Lys-D-Ala-D-Ala **1** and **b**, **2**. Dotted lines represent hydrogen bonds, wavy lines represent more than one intervening bond of the antibiotic.

indicate that each proton is present in several magnetically distinct environments corresponding to two forms of a back-to-back dimer and a small population of antibiotic monomer that are slowly interconverting.[7–9] Resonances corresponding to this complex mixture have been partially assigned and characterised previously in several solvents, with several bound ligands.[7–9,11] The highfield region of the 1D ^{1}H NMR spectrum of ristocetin A (Fig. 3i, 0 to 3 ppm) demonstrates the existence of slowly exchanging monomer (M) and two forms of the dimer (D1 and D2) for the methyl group of the rhamnose sugar (**Rh$_6$**) of the tetrasaccharide attached at residue 4 of the antibiotic (see Fig. 2). In contrast, the complex of compound **2** with ristocetin A under the same experimental conditions presents a considerably simplified ^{1}H NMR spectrum. Notably, the Rh$_6$ resonance is shifted upfield by approximately 1 ppm compared with the monomer shift for ristocetin A, and exists in a single chemical environment (Fig. 3ii). A magnetisation transfer study on a mixture of free and bound antibiotic (3:1 ratio of ristocetin A:ligand; Fig. 3iii) is shown in Fig. 3iv; irradiating the resonance at δ 0.18, corresponding to Rh$_6$ in the complex, results in transfer of saturation to the free antibiotic resonances of Rh$_6$ in the monomer (M), and dimer forms (D1 and D2), confirming the assignment of the Rh$_6$ resonance in the complex at δ 0.18, and identifying slow exchange between the bound and the free antibiotic under these conditions. Further, the large ligand-induced upfield shift of Rh$_6$ is indicative of its close proximity to the face of an aromatic ring, subsequently shown to be that of the bound ligand.

Assignment of the ^{1}H resonances of the ristocetin A–compound **2** complex is achieved partially through coherence transfer correlations identified in TOCSY spectra (to identify spin systems of the amino acid side chains and sugar residues *via* spin-spin coupling interactions), and through-space dipolar interactions identified in NOESY spectra, collected with mixing times of between 20 and 400 ms. Chemical shift values and important NOEs are collated in Table 1. ^{1}H NOESY data

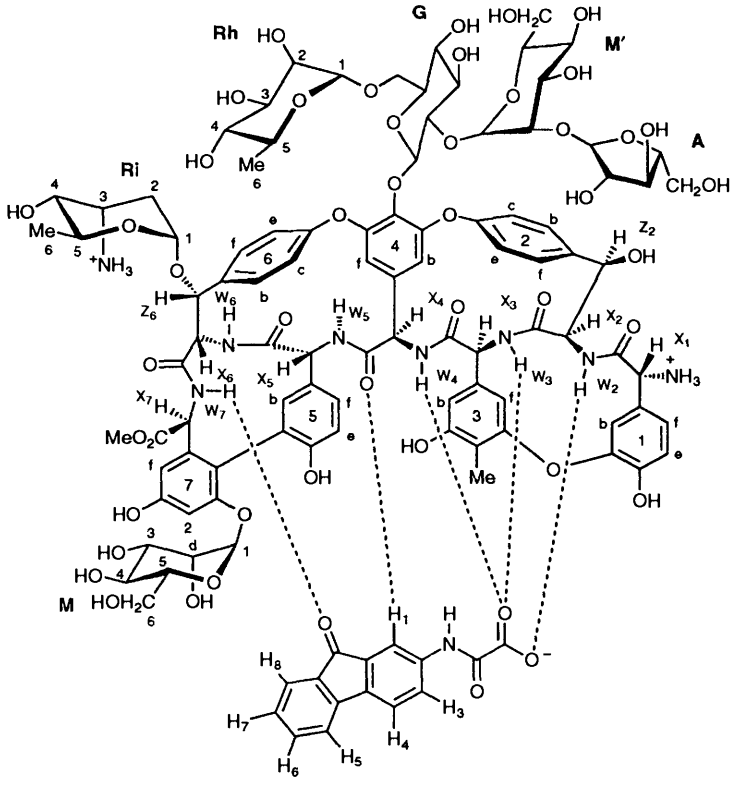

Fig. 2 Structure of the complex identifying antibiotic sugar residues involved in ligand binding; **Ri** (ristosamine), **Rh** (rhamnose). Other sugars include **M** (mannose), **A** (arabinose), **G** (glucose). Dotted lines represent intermolecular hydrogen bonds.

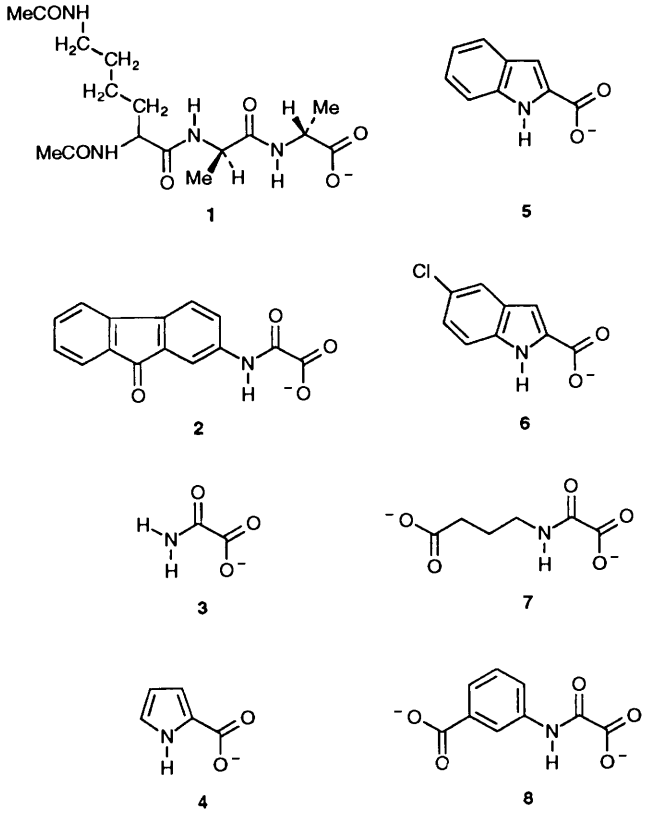

Scheme 1

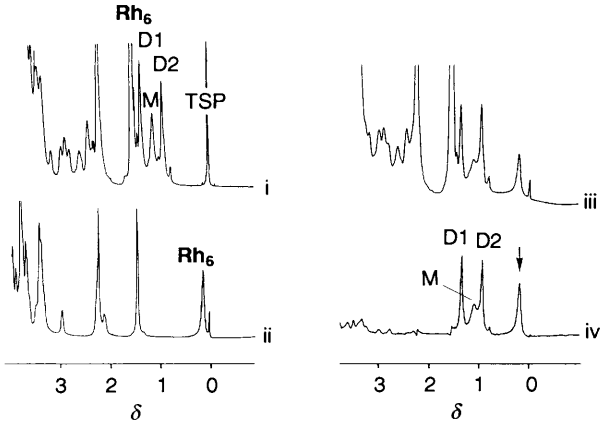

Fig. 3 500 MHz 1D ^{1}H NMR spectra (*ca.* 0.0 to 3.0 ppm) of i, ristocetin A, ii, 1:1 complex of ristocetin A with ligand **2**, iii, 3:1 mixture of ristocetin A:ligand **2**, and iv, difference spectrum from on and off-resonance irradiation of Rh_6 resonance δ 0.18 in spectrum iii. An arrow in iv identifies the irradiated resonance. Spectra were recorded at 288 K, pH 7.0. In spectrum i, M, D1 and D2 correspond to the Rh_6 resonances due to antibiotic monomer, and the two forms of the dimer, respectively (see text).

Table 1 Chemical shift assignments and observed NOEs in the ristocetin A complex with compound **2**

Proton	Chemical shift (ppm)[a]	NOEs observed[b]
x_1	5.33	1, 1f, 2f, 3b
x_2	5.41	z_2, 2b
z_2	5.59	x_2, 2b, 2c, 2f
x_3	5.54	3b, 3f
3-Me	2.19	1b, 3b, M'$_1$, M'$_2$
x_4	5.59	4b, 4f
x_5	4.93	x_6, z_6, 5b, H_1
x_6	3.89	x_5, 5b, z_6, 6b, 4f, H_1
z_6	4.50	x_6, 6b, Rh_6, Ri_1, Ri_5, Ri_6, 5b, 6c, H_7, H_8
CO_2Me	4.09	7f, Ri_6, H_7, H_8
Rh_1	4.26	
Rh_2	3.68	
Rh_3	3.34	
Rh_4	2.91	
Rh_5	2.21	6b, 6c
Rh_6	0.18	z_6, 6b, 6c, H_4, H_5, H_6, Ri_1, Ri_6, 6f
Ri_1	4.78	z_6, Rh_6
Ri_2	2.07	
Ri_2'	2.22	
Ri_3	3.71	
Ri_4	3.61	
Ri_5	3.27	z_6
Ri_6	1.41	z_6, CO_2Me, Rh_6, 7f, H_7, H_8
M'$_1$	5.76	7d, 3-Me
M'$_2$	3.64	3-Me, 7d
M'$_3$	3.35	7d
1b	6.83	x_1, 3b, 3-Me
1e	6.87	1f, H_3, H_4
1f	7.29	x_1, 1e, H_3, H_4
2b	7.23	x_2, z_2, 2c, 4b
2c	7.37	z_2, 2b, 4b
2e	7.34	2f
2f	7.91	x_1, z_2, 2e
3b	6.89	1b, x_3, 3f, 3-Me
3f	6.65	x_3, 3b
4b	6.19	2b, 2c, x_4
4f	5.15	x_4, 5b, x_6, 6c, 6e
5b	8.22	x_5, x_6, z_6, 4f, 6b, 5f, H_1
5e	7.04	5f
5f	7.15	5e, 5b
6b	5.99	z_6, 6c, Rh_5, Rh_6, x_6, 5b, H_1, H_7, H_8
6c	5.65	4f, 6b, z_6, Rh_5, Rh_6, H_1
6e	7.12	4f, 6f
6f	7.28	6e, Rh_6
7d	7.05	M'$_1$, M'$_2$
7f	6.77	CO_2Me, Ri_6, H_7, H_8
Ligand assignments		
H_1	7.72	x_6, x_6, 5b, 6b, 6c
H_3	8.62	1e, 1f
H_4	7.56	Rh_6, 1e, 1f
H_5	6.93	Rh_6
H_6	6.51	
H_7	7.39	CO_2Me, Ri_6, z_6, 6b, 7f
H_8	7.35	CO_2Me, z_6, 6b, 7f, Ri_6
NH_L	9.03	

[a] Chemical shifts at 15 °C, sample concentration $\approx$5 mmol dm^{-3}. [b] Intra-saccharide NOEs are not included.

collected in H_2O–D_2O (9:1) solutions of the complex, at pH 4.5 and 283 K (Fig. 4), have also enabled the amide NHs (w_2 through to w_7) to be assigned, as indicated in Table 2. NOEs involving several of these latter resonances, together with their temperature dependent shifts, have been particularly useful in confirming interactions in the ristocetin binding site, as discussed below. The NH of the bound ligand (NH_L) is readily identified at δ 9.03, giving a strong intramolecular NOE to H_1 on the adjacent fluorenone ring. Several specific NOE cross-peaks from amide NHs are identified in Fig. 4 and the data are collated in Table 2.

Chemical Shift Perturbations and Hydrophobic Interactions.—Many proton resonances from the antibiotic undergo large ligand-induced chemical shift changes that are diagnostic of the site of binding and ligand orientation. The effects of ligand binding on the chemical shift values of the protons on the aromatic side chains of ristocetin A (versus those in the monomeric ristocetin)[11] are summarised graphically in Fig. 5

Table 2 Chemical shifts (δ) and temperature coefficients (δ/T in ppb K^{-1}) for amide NHs of ristocetin A in the ligand-free antibiotic and when complexed with compound **2** and di-*N*-Ac-L-Lys-D-Ala-D-Ala **1**

		2–complex		1–complex[a]	
Proton	δ, free[a]	$\delta^{a,c}$	δ/T[d]	δ^{b}	δ/T
w_2	7.94	10.76 (−2.82)	−0.8	11.61 (−3.67)	−1.4
w_3	7.44	9.18 (−1.74)	—	9.72 (−2.88)	−0.6
w_4	8.33	8.82 (−0.49)	−0.1	9.43 (−1.1)	−1.0
w_5	9.24	9.20 (0.04)	−8.4	9.23 (0.01)	−7.0
w_6		8.11 (−)	−11.4		
w_7	9.55	9.67 (−0.12)	−5.2	9.58 (−0.03)	−0.7

NOEs from antibiotic amide NHs in **2**-ristocetin complex[e]

NH	NOEs	NH	NOEs	NH	NOEs
w_2	w_3, 2f, z_1	w_3	w_2, w_4, 2f, 3b	w_4	w_3, 3b, 4b
w_5	x_4, 4f, 5f	w_6	6e, 6f, x_6	w_7	5b, x_6, H_8

[a] pH 4–5, 293 K (data from ref. 11); [b] values in parentheses represent ligand-induced changes in chemical shift ($\delta_{free}-\delta_{bound}$); [c] pH 4.5, 283 K; [d] determined from linear slope of δ vs T for 8 data points between 278 K and 293 K; [e] 2D NOESY data at 283 K, pH 4.5.

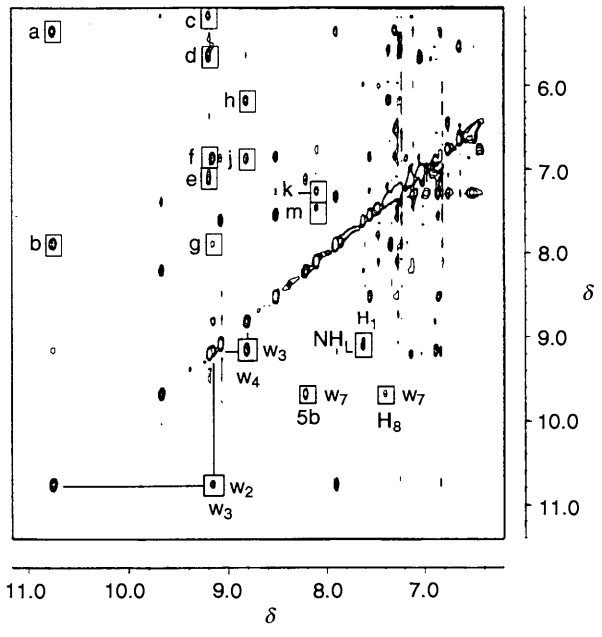

Fig. 4 Portion of the 500 MHz NOESY spectrum (mixing time 300 ms) of the Ristocetin A– compound **2** complex recorded in H_2O–D_2O (9:1), pH 4.5 and at 283 K. This region of the spectrum highlights the NOE cross peaks involving the exchangeable amide NH protons (w_2, w_3, w_4, w_5, w_6 and w_7). Several individual cross peaks are labelled as follows: a w_2–2f; b w_2–x_1; c w_5–4f; d w_5–x_4; e w_5–5f; f w_3–3b; g w_3–2f; h w_4–4b; j w_4–3b; k w_6–6e; m w_6–6f.

for complexation with the compounds **1** and **2**. Particularly large chemical shift perturbations (both upfield and downfield) to protons on the side chains of resdues 5 and 6 identify the fluorenone moiety as binding in close proximity to these residues. Protons 6b and 6c appear to be located directly over the π-face of the bound ligand, undergoing upfield shifts of 1.47 and 1.28 ppm, respectively. In contrast, proton 5b undergoes a large downfield shift of 1.22 ppm, indicative of a predominant orientation that lies near to the plane of the fluorenone ring system on the floor of the binding pocket (see Fig. 2). The large upfield ring-current shift experienced by Rh_6 ($\Delta\delta$ = 0.91 ppm), indicates that the rhamnose sugar is binding in close contact with one hydrophobic face of the fluorenone π-system. NOEs

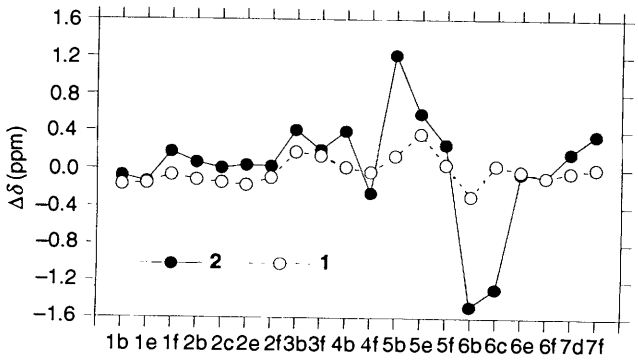

Fig. 5 Effect of binding **1** and **2** on the ^1H chemical shift values of the aromatic protons of ristocetin A. Chemical shift changes are with reference to those reported in ref. 11.

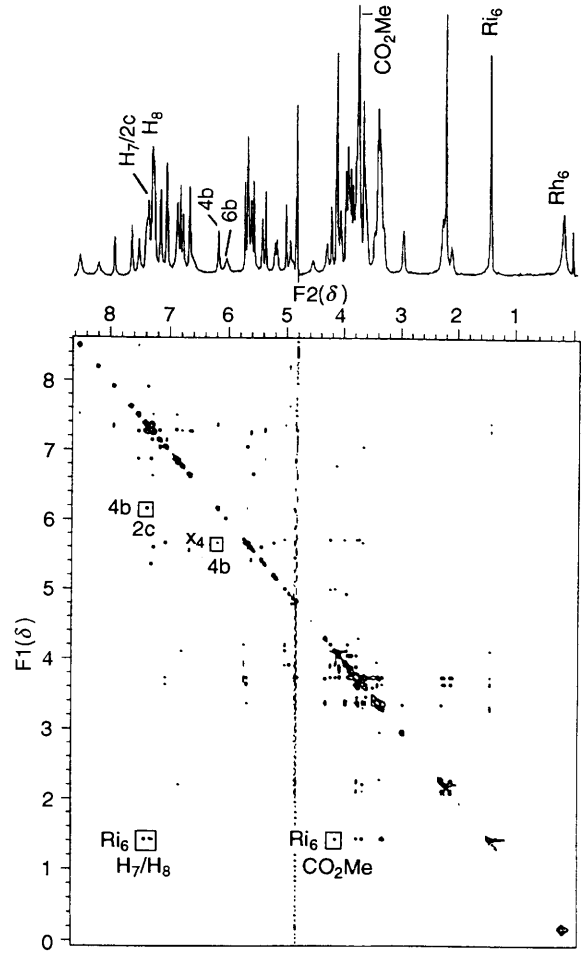

Fig. 6 NOE data at 600 MHz (50 ms mixing time) illustrating short-range interactions in the complex of ristocetin A with compound **2**. A number of NOEs referred to specifically in the text are labelled.

between Rh_6 and H_6/H_7 of the ligand are consistent with this interaction, while NOEs between Rh_6 and 6b/6c of the antibiotic place Rh_6 in contact with the top edge of the aromatic side chain of residue 6. Additional hydrophobic interactions are manifested in the form of intermolecular NOEs between the methyl group of the ristosamine sugar (Ri_6) and ligand protons H_7 and H_8, and from the methyl ester of the terminal residue to H_7 and H_8. The former NOEs, involving Ri_6, correspond to particularly short range interactions and are readily detected in the 50 ms NOESY spectrum (Fig. 6). Moreover, NOEs between Ri_6–Rh_6 and Ri_6–CO_2Me (Fig. 6), identify

Table 3 Selected proton–proton distances (Å) determined from the energy minimised structure of the complex of compound **2** with ristocetin A[12]

Ligand–antibiotic			
Rh_6–H_6	4.5	Ri_6–H_7	3.4
CO_2Me–H_8	3.6	Ri_6–H_8	4.0
5b–H_1	2.4	w_7–H_8	3.2
Hydrophobic 'wall'			
Rh_6–Ri_6	4.4	CO_2Me–Ri_6	2.6
Ri_6–z_6	3.3		

Table 4 ^1H chemical shift values (δ at 298 K) for selected aromatic protons that are diagnostic of antibiotic dimerisation[7]

	Ristocetin–**1** complex		Ristocetin–**2** complex
Proton	Monomer	Dimer	
6e	7.38	5.09/5.18	7.14
6f	7.51	6.81/6.70	7.29

a hydrophobic 'wall' of methyl groups against which one face of the ligand is able to bind. All of these NOEs are consistent with the structural modelling studies described below (Table 3).

A number of additional conformational features of the complex are evident from semi-quantitative interpretation of NOE data. The aromatic rings of residues 2 and 6, which are roughly orthogonal to ring 4 (Fig. 2), produce upfield ring current shifts on 4b and 4f of unbound ristocetin; NOEs from 4b and 4f to x_4 suggest similar average distances of these two aromatic protons to x_4. In the presence of the ligand **2**, residue 4 adopts a different preferred conformation, as suggested by a stronger NOE for x_4–4b, than for x_4–4f. Additionally, 4b now shows NOEs to 2c and 2b, and is shifted downfield 0.4 ppm, consistent with a change in conformation such that 4b is no longer directly underneath the aromatic ring of residue 2. Similarly, 4f appears to change its orientation with respect to ring 6, undergoing an upfield shift of 0.25 ppm.

Compound **2** *Binds Anti-cooperatively to the Ristocetin A Dimer.*—Previous ^1H NMR studies have shown that protons 6e and 6f (Fig. 2) undergo large dimer-induced upfield shifts of *ca.* 2.2 and 0.7 ppm, respectively,[7,8] as a consequence of their orientations over the face of ring 4 of the dimer partner, and these changes are considered diagnostic of antibiotic dimerisation. The proposed hydrogen bonding pattern between the two halves of the dimer is illustrated in Fig. 7. The chemical shifts of 6e and 6f in the ristocetin A complex with compound **2**, when compared with those in the monomer and dimer forms of the complex of ristocetin A with tripeptide **1**[7] (Table 4), indicate convincingly that compound **2** is bound to the monomeric form of the antibiotic. Both 6e and 6f have small upfield shifts of < 0.25 ppm compared with the ristocetin–tripeptide monomer complex,[7] consistent with small ring-current contributions from the bound fluorenone ligand. Additionally, NOEs between the two halves of the dimer (Ri_2/Ri_2'–2c; Ri_2/Ri_2'–x_3; Ri_3–x_3; 6f–4b), also regarded as diagnostic of the back-to-back dimer, but inconsistent with the monomeric structure, are absent from the NOESY spectra of the complex of **2**.

Hydrogen Bonding Interactions.—The resonances of amide protons (w_2, w_3 and w_4) involved in direct hydrogen bonding to cell-wall fragments undergo large downfield shifts characteristic of shielding effects from the ligand carboxylate group.[11] The effect is particularly pronounced for w_2, which shifts downfield by *ca.* 3.6 ppm when di-*N*-Ac-L-Lys-D-Ala-D-Ala binds to ristocetin A, although substantial shifts (> 1 ppm) are

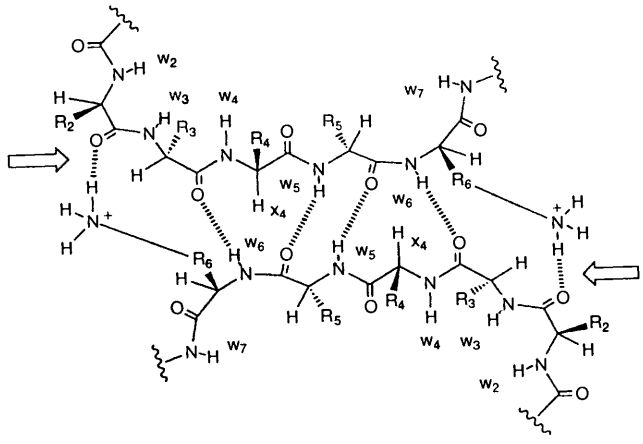

Fig. 7 Intermolecular hydrogen bonding interactions between monomer units in the proposed model of the back-to-back dimer of ristocetin A.[7] Interactions involving the ristosamine charged amino group of one monomer and the carbonyl oxygen of residue 2 of the second monomer are highlighted; this interaction occurs twice in the dimer.

observed for all amide NHs located in the carboxylate binding pocket. Similarly large effects are observed for ristocetin A in the complex with compound **2**, particularly for w_2 which has a similarly large downfield shift of ≈2.8 ppm, providing strong evidence that compound **2** is located in the antibiotic binding pocket and is interacting in the manner represented schematically in Figs. 1 and 2. Several intermolecular NOEs support such a hydrogen bonding scheme; for example, ligand proton H_1 points into the binding pocket (see Fig. 2) and gives an NOE to 5b, whilst an NOE between w_7 and ligand H_8 supports a hydrogen bonding interaction between the fluorenone carbonyl group and w_7 (Fig. 2). The alignment of the three antibiotic amide NHs (w_2, w_3 and w_4) that bind the ligand carboxylate, as depicted in Figs. 1 and 2, is clearly evident from the pattern of sequential NOEs from w_2–w_3–w_4 (see Fig. 4). Amide NH chemical shift values and NOE data are summarised in Table 2. The temperature coefficients for these protons (with the exception of the obscured w_3), have also been measured and are worthy of note. The amide NH protons w_2 and w_4 are inaccessible to solvent through hydrogen bonding to the carboxylate group of compound **2**, and have very small temperature coefficients (< 1.0 ppb K^{-1} in both cases, and similar to those reported for di-*N*-Ac-L-Lys-D-Ala-D-Ala binding to ristocetin A).[7] A similarly small temperature coefficient for NH_L of 1.7 ppb K^{-1} is also consistent with its involvement in intermolecular hydrogen bonding (Fig. 2). In contrast, w_5 and w_6 have much larger coefficients of 8.4 and 11.4 ppb K^{-1}, respectively, indicative of exposure to the solvent on the back face of the antibiotic. This latter observation provides further evidence for a monomeric complex. In the proposed structure of the back-to-back dimer of ristocetin A (Fig. 7), w_5 and w_6 are involved in intermolecular hydrogen bonds and have been shown to have characteristically small temperature coefficients.[9] In the extreme case of eremomycin, which dimerises strongly (K_{dim} > 10^6 dm^3 mol^{-1}), the corresponding NHs also have very slow exchange kinetics, consistent with shielding from the solvent.[9]

Structure of the Complex of **2** *with Ristocetin A.*—An energy minimised structure of the complex has been generated using the molecular mechanics program MacroModel,[12] for comparison with the NMR data described above. Selected proton-proton distances measured from this minimised structure are presented in Table 3. The general features discussed above in the qualitative description of the binding interaction, are

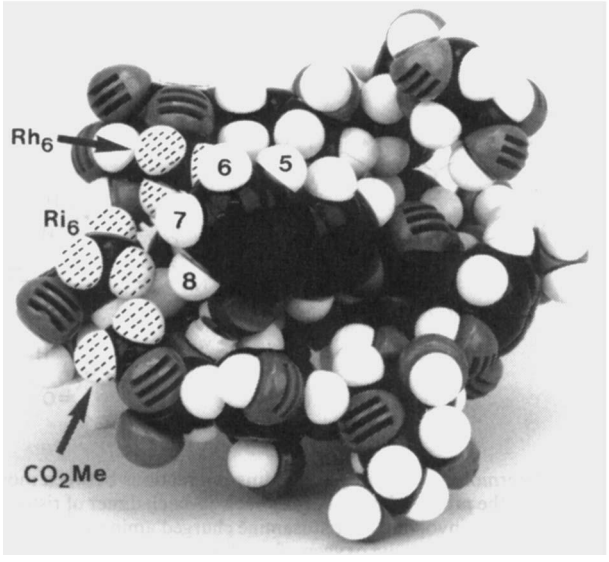

Fig. 8 CPK model of the complex of compound **2** with ristocetin A monomer. The antibiotic methyl groups Rh_6, Ri_6 and CO_2Me are highlighted (labelled and hatched). Ligand protons H5, H6, H7 and H8 are numbered.

Table 5 Dimerisation constants (K_{dim}) and dimerisation free energies ($\Delta G°_{dim}$) for ristocetin A at 298 K in the presence and absence of ligands

Ligand	K_{dim}/mol^{-1}	$\Delta G°_{dim}$/kJ mol^{-1}
no ligand	500	−15
1	350[b]	−14
2	<1[c]	<0
3	600	−16
4	600	−16
5	≈20	≈−7
6	≈10	≈−5
7	700	−16
8	100	−11

[a] Estimated errors ± 20%. [b] Determined from the relative intensities of the bound resonances of the ligand C-terminal alanine methyl group in monomer and dimer conformation; estimated error ± 10%. [c] Too small to determine, no detectable amount of dimer present at 20 mmol dm^{-3} total concentration of antibiotic.

consistent with this partially refined structure. In Fig. 8, the binding interaction with the hydrophobic 'wall' of methyl groups comprising Rh_6, Ri_6 and the methyl ester of residue 7, is most clearly illustrated using CPK models. The strong intermolecular NOEs identified between Ri_6 and ligand protons H_7 and H_8 correspond to interproton distances in the energy minimised structure (Ri_6–H_7, 3.4 Å; Ri_6–H_8, 4.0 Å) that are consistent with the experimental NOEs. It is estimated that the total hydrophobic surface area buried (both ligand and antibiotic) from access to solvent is ≈204 Å^2, a value similar to that estimated for the binding of *N*-Ac-D-Ala-D-Ala (≈215 Å^2), indicative of very similar hydrophobic contributions to binding.[5] It should be noted that these hydrophobic interactions arise, in large part, from unnatural interactions in the sense that binding the natural substrate does not involve direct contacts with the ristosamine and rhamnose sugars.

The Role of Antibiotic Sugars in Ristocetin A Dimerisation.—It has been established that the sugar substituents of ristocetin A play an important role in promoting dimerisation.[8] The estimated dimerisation constant for ristocetin A of between 300–500 dm^3 mol^{-1} at 298 K from earlier studies,[8] and this work (see below), is reduced to ≈50 dm^3 mol^{-1} when the residue 7 mannose and residue 4 tetrasaccharide are removed simultaneously by acid methanolysis.[8] Similarly, a 100-fold reduction in K_{dim} is observed upon removal of the disaccharide of eremomycin.[8] While the nature of the involvement of the residues 4 and 7 sugars in promoting dimerisation remains to be firmly established, the ristosamine sugar on residue 6 has been directly implicated in interactions at the dimer interface. For example, intermolecular NOEs have been detected between ristosamine sugar protons of one monomer unit and 2c and x_3 of its partner in the dimer;[7] these NOEs are incompatible with the structure of the antibiotic monomer, and are indicative of possible van der Waals contacts at the dimer interface. Moreover, the charged amino group of the ristosamine sugar appears to be suitably oriented to form a direct intermolecular hydrogen bond to the backbone carbonyl of residue 2 (Fig. 7). We now attempt a semi-quantitative dissection of ligand–antibiotic interactions that appear to be influential in perturbing the monomer ⇌ dimer equilibrium. We have considered the effects of binding a series of ligands on ristocetin A dimerisation; several of these ligands approximate to truncated analogues of compound **2**, and allow a semi-quantitative, stepwise assessment of anti-cooperative binding contributions.

Stepwise Analysis of Anti-cooperative Binding.—The compounds considered are shown in Scheme 1; values for the dimerisation constant K_{dim} and the corresponding free energy of dimerisation $\Delta G°_{dim}$ (298 K) are presented in Table 5. The extent of antibiotic dimerisation has been monitored from the effects of added ligand on the signal intensities of the rhamnose methyl (Rh_6) in the monomer and dimer forms of the antibiotic. The M, D1 and D2 signals have already been highlighted for the uncomplexed ristocetin A in Fig. 3i. In the case of the di-*N*-Ac-L-Lys-D-Ala-D-Ala complex, K_{dim} was estimated from the relative intensities of the resolved signals of the ligand C-terminal Ala methyl group in the monomer and dimer bound states. The ligand concentrations employed in these experiments ensured that the antibiotic was >95% complexed. (Details of estimated ligand binding constants and detailed NMR studies of these complexes will be described in a subsequent publication.) While compounds **3** and **4** have essentially the same affinity for monomer and dimer, indole-2-carboxylic acid **5**, in contrast, binds more strongly to the monomeric ristocetin A, with a specificity for monomer over dimer estimated to be ≈25 from the ratio of K_{dim} values for ligand-free antibiotic and complex (see Table 5). While compounds **3** and **4** have a relatively minor effect on the monomer ⇌ dimer equilibrium, introducing the large hydrophobic aryl ring of the indole-2-carboxylic acid **5** (or the 5-chloro analogue **6**), has a pronounced anti-cooperative effect on dimerisation (Table 5). The NOE data shed some light on the interaction of ristocetin A with compound **5**. Cross-peaks in 2D spectra (data not shown) are readily identified between protons on the upper edge of the indole ring (H_4 and H_5) and Rh_6 on the residue 4 tetrasaccharide of the antibiotic. These NOEs are analogous to those identified between compound **2** and ristocetin A, but have no counterpart in complexes with the natural substrate, di-*N*-Ac-L-Lys-D-Ala-D-Ala,[11] which lacks an aromatic ring. Models of the ristocetin A complex with compound **5** indicate that the indole ring system is unable to extend as far along the binding cleft as the fluorenone moiety; consequently, no intermolecular interactions were anticipated between ligand protons and ristosamine methyl and residue 7 methyl ester (proton-proton distances >5 Å), and indeed, no such NOEs were detected. We conclude that the ristosamine sugar is probably unperturbed by the binding of the indole ligands, and appears likely to be able to participate in interactions at the dimer interface as indicated in Fig. 7. Thus, the observed anti-cooperative effect of binding compound **5** to the dimer, is somewhat less than observed for

compound **2** (> 500), perhaps as a consequence of some proportion of the ristosamine contribution to dimerisation.

Previously, we have reported the rational design and binding of the 4-carboxylatocarbonylaminobutanoic acid **7** to ristocetin A.[10] NMR studies of the complex confirm that the oxalate group binds in the carboxylate binding pocket of the natural substrate, with the butanoic acid side-chain orientated as required by hydrogen bonding of its butanoic carboxylate function to w_7 of the antibiotic. This orientation is indicated by NOEs from the methylene protons to protons of residue 5 and 6 that form the hydrophobic alanine methyl binding pocket of the cell wall analogue (data not shown). Thus, compound **7** exhibits a complementarity for the antibiotic binding pocket that closely mimics the cell wall analogue di-*N*-Ac-L-Lys-D-Ala-D-Ala. In the present study, both ligands **1** and **7** are found to have quite small effects on antibiotic dimerisation (see Table 5). It appears that binding of cell wall components (and *close* analogues) and antibiotic dimerisation are compatible phenomena, and perhaps, therefore, likely to play an important role in the mode of antibiotic action. Although the dimerisation process is found to be slightly anti-cooperative in the presence of the natural substrate, dimerisation becomes *highly* anti-cooperative when distinctly non-natural ligands are introduced. By comparison, dimerisation of vancomycin, which is the most clinically important member of this group, is promoted to a small degree by a substrate analogue (factor of ≈2).[9] Eremomycin has the largest dimerisation constant ($\approx 10^6$ dm^3 mol^{-1}) so far determined, and also shows the largest enhancement of dimerisation by substrate binding (a factor of 100). Interestingly, the activity of eremomycin is approximately 2–5 times higher than for vancomycin, suggesting some specific role for dimerisation in the mechanism of action of these antibiotics.[9]

Conclusions

The ligands described in this paper, particularly those that bind through 'non-natural' interactions with the antibiotic (*i.e.*, those structures incorporating bulky aromatic rings), perturb the finely honed complementarity between ligand and receptor through interaction with the saccharides of residues 4 and 6, which are also crucial for the formation of the dimer complex. The consequence is that the binding of these ligands and dimerisation are highly anti-cooperative phenomena. The conformational changes produced by the fluoroenone moiety, and to a lesser extent the indole ring system, must introduce favourable free energy contributions to ligand binding (hydrophobic effect, van der Waals interactions, π-stacking interactions) that more than offset the loss of free energy from dimerisation. Ligand **2** binds to the ristocetin A monomer with such high specificity (> 500) that even at saturating concentrations of complex (≈20 mmol dm^{-3}), no dimer is detected (implying K_{dim} < 1 dm^3 mol^{-1}). Studies with the indole ligand **5** suggest that interactions with the rhamnose sugar of the tetrasaccharide and subsequent perturbations to its orientation with respect to the dimer interface, may be responsible for a factor of ≈25 in specificity for monomer. The interaction of the fluorenone ring with the ristosamine sugar may, therefore, contribute at least an additional factor of 10 in specificity, perhaps through disruption of two charged hydrogen bonding interactions at the dimer interface (Fig. 7). The NOE data on the ristocetin A complex with compound **2** show convincingly that the pendant sugars of the antibiotic monomer are 'organised' into a hydrophobic wall which the ligand exploits in binding, but which is evidently incompatible with the complementarity required for back-to-back dimerisation.

Experimental

Materials.—Ristocetin A was a gift from Lundbeck (Copenhagen) and was used without further purification. *N*-(9-Oxofluoren-2-yl)oxamic acid **2** was prepared as follows. Methyloxalyl chloride (1 equiv.) was added to a solution of 2-aminofluorenone (1 equiv.) and *N*-methylmorpholine (1 equiv.) in dichloromethane (20 cm^3) and the mixture was stirred at room temperature for 4 h. The resulting solution of the methyl ester of **2** was washed with aqueous citric acid (0.1 mol dm^{-3}), saturated aqueous sodium hydrogencarbonate and water, and then recovered from the dichloromethane by rotary evaporation under reduced pressure. Hydrolysis of the methyl ester of **2** with aqueous lithium hydroxide (10 equiv.) yielded the product **2**. Purification on a Dowex-50 ion exchange resin gave the free acid of **2**, which crystallised from water–methanol (1 : 1) as fine yellow needles.

All other ligands were purchased from Aldrich Chemical Company (and used without further purification), or synthesised as previously described (ligands **7** and **8**).[10]

Methods.—1D and 2D ^{1}H NMR spectra were collected on Bruker AM 500 and Varian Unity 600 spectrometers. NOESY spectra in H_2O–D_2O solutions (9 : 1) were collected at 500 MHz using a 1-1 binomial 'read' pulse to give selective suppression of the solvent resonance. 500 MHz 2D spectra were collected as 1K data points for 320 t_1 increments (using the TPPI method), zero-filled to a 2K × 2K matrix prior to fourier transformation using sinebell-shifted window functions in both t_1 and t_2. 600 MHz NOESY and TOCSY spectra were collected as 2K × 300–400 t_1 increments and zero-filled to 2K × 2K prior to transformation. Data were processed on a Sun data station with VNMR software.

Acknowledgements

We thank SERC for financial support. P. G. would like to thank Xenova and SERC for a CASE Studentship. We are grateful to Dr. J. P. MacKay for helpful discussions on various aspects of this work.

References

1 J. C. Barna and D. H. Williams, *Ann. Rev. Microbiol.*, 1984, **38**, 339.
2 G. M. Sheldrick, P. G. Jones, O. Kennard, and D. H. Williams, *Nature*, 1978, **271**, 223.
3 D. H. Williams, *Acc. Chem. Res.*, 1984, **17**, 364.
4 D. H. Wiliams, J. P. L. Cox, A. J. Doig, M. Gardner, U. Gerhard, P. T. Kaye, A. R. Lal, I. A. Nicholls, C. J. Salter and R. C. Mitchell, *J. Am. Chem. Soc.*, 1991, **113**, 7020.
5 M. S. Searle, D. H. Williams and U. Gerhard, *J. Am. Chem. Soc.*, 1992, **114**, 10 967.
6 D. H. Williams, M. S. Searle, J. P. Mackay, U. Gerhard and R. A. Maplestone, *Proc. Natl. Acad. Sci. USA*, 1993, **90**, 1172.
7 J. P. Waltho and D. H. Williams, *J. Am. Chem. Soc.*, 1989, **111**, 2475.
8 U. Gerhard, J. P. Mackay, R. A. Maplestone and D. H. Williams, *J. Am. Chem. Soc.*, 1993, **115**, 232.
9 J. P. Mackay, U. Gerhard, D. A. Beauregard, R. A. Maplestone and D. H. Williams, submitted for publication.
10 S. E. Holroyd, P. Groves, M. S. Searle, U. Gerhard and D. H. Williams, *Tetrahedron*, 1993, **49**, 9171.
11 M. P. Williamson and D. H. Williams, *J. Chem. Soc., Perkin Trans. 1*, 1985, 949.
12 F. Mohamadi, N. G. J. Richards, W. C. Guida, R. Liskamp, M. Lipton, C. Caufield, G. Chang, T. Hendrickson and W. C. Still, *J. Comput. Chem.*, 1990, **11**, 440.

Paper 3/06140J
Received 14*th October* 1993
Accepted 22*nd October* 1993